Effects of ion irradiation on conductivity of $CrSi_2$ thin films

T. C. Banwell, X.-A. Zhao,[a] and M-A. Nicolet
California Institute of Technology, Pasadena, California 91125

(Received 21 October 1985; accepted for publication 14 January 1986)

Electrical resistivity measurements are used to study damage in $CrSi_2$ thin films induced by Ne, Ar, or Xe ion irradiation over a fluence range of 10^{10}–10^{15} ions cm^{-2}. Irradiation produces a factor of 5–12 increase in film conductivity at the higher fluences. The influence of defect generation and recombination is evident. We speculate that formation of a compound defect is a dominant factor enhancing film conductivity. A temperature dependence at low fluences is reported and tentatively identified.

I. INTRODUCTION

The use of metal silicides in contact and interconnect technologies has motivated investigation of irradiation damage in silicides.[1–3] Recent studies show that the electrical conductivity of $CoSi_2$, $NiSi_2$, and Pd_2Si films are lowered by ion irradiation,[1,2] presumably due to the reduction in carrier mobility. In contrast, the conductivity of $CrSi_2$ can be increased by ion irradiation.[2,3] The details of the responsible processes are unknown. $CrSi_2$ is particularly interesting since it is a narrow (0.27 eV) band-gap semiconductor.[4,5] Thermally grown $CrSi_2$ films typically show degenerate p-type conductivity with carrier densities exceeding 10^{20} cm^{-3}. Electron and hole mobilities are 0.15 and 15 cm^2/V s, respectively.[4]

We report here on our investigations of changes in electrical transport in $CrSi_2$ films associated with Xe, Ar, and Ne ion irradiation. Two models are proposed which offer some insight into the damage process.

II. EXPERIMENT

$CrSi_2$ films were produced on several types of substrates. Approximately 1-μm-thick SiO_2 layers were thermally grown on 0.01 Ω cm n-type $<111>$ Si wafers by wet oxidation. Following oxidation, 80-nm Si, 40-nm Cr, and 40-nm Si layers were sequentially deposited thereon by e-beam evaporation; the background pressure remained below 10^{-7} Torr. Also, 30–50 Ω cm n-type $<100>$ Si and 5–30 Ω cm p-type $<111>$ Si wafers were organically cleaned, etched in 10% HF, slightly oxidized in boiling [H_2O_2, NH_3 (aq), H_2O: 1,1,5] and finally dipped in 3% HF prior to loading for deposition. Consecutive depositions of 40-nm Cr and 20-nm Si were made on these substrates. The Si cap was employed to minimize oxygen contamination. All samples were sequentially annealed at 600 °C, 30 s and 900 °C, 60 s in vacuum at $<7\times10^{-7}$ Torr. 2-MeV He backscatter spectrometry and x-ray diffraction (Read camera) were used to characterize the stoichiometry and structure of sections of each wafer. This showed the formation of 120-nm $CrSi_2$ in each case.[4] A slight (<10 nm) excess of Si was present at the surface of the samples on SiO_2. The samples were cleaved into 8×8 mm squares and electrically characterized before further use by four-point probe measurements of sheet resistance and Hall coefficient at room temperature, using standard methods.[6] There was negligible substrate conduction in the samples on the n-type $<100>$ Si or SiO_2 substrates; these $CrSi_2$ films were p-type with typical resistivities of ~4400, ~5500 $\mu\Omega$ cm, carrier concentrations of ~1, $\sim2\times10^{20}$ cm^{-3}, and Hall mobilities of ~13, ~7 cm^2/V s, respectively. The substrate contributed $\sim50\%$ to the measured film conductivity in the samples on the p-type $<111>$ Si wafer.

Two complementary irradiation experiments were performed. In one, samples were irradiated at room temperature (RT) with Xe at energies of 300–600 keV to fluences of 10^{11}–10^{15} Xe cm^{-2} at particle current densities, corresponding to a singly charged ion, of 2–100 nA/cm^2. The irradiated films were then characterized as before. The second set of experiments employed four-point electrical resistivity measurements of $CrSi_2$ films on SiO_2 made *in situ* with 300–500-keV Xe irradiation at room temperature and 77 K. Measurements were made for accumulated doses of 2×10^{10}–10^{15} ions cm^{-2}. Constant particle current density was maintained during irradiation, typically in the range 0.8–5 nA/cm^2. The relative uncertainty in dosimetry was $<1\%$ for a given run, and the absolute uncertainty was estimated to be $<10\%$. Similar implantations with 150-keV Ar and 90-keV Ne at room temperature were also performed.

Except for the 600-keV Xe irradiation, the (mean damage depth) + (damage straggling)$^{1/2}$ was less than the 120-nm $CrSi_2$ film thickness for all ions and energies used.[7] A thin film of thermally conductive paste (Dow Corning 340) was used to secure the samples to an implantation carousel of large thermal mass. We estimate the sample temperature to have risen less than 0.01 °C/nA cm^{-2}.

III. RESULTS

$CrSi_2$ film conductance increases with incident ion fluence ϕ for room- temperature Xe and Ar irradiation. Samples irradiated with Xe at 77 K, or with Ne at RT initially display a $\sim2\%$ decrease in conductance at fluences $<10^{11}$ cm^{-2}, beyond which the conductivity also increases with fluence. The film conductance $g(\phi)$ saturates at 5–12$\times$ its initial value g_0 for fluences of 6×10^{13}–10^{15} cm^{-2}. The apparent saturation level increases when larger particle current densities are employed. Additional investigations indicate that this is not the result of Joule heating.

Typical *in situ* results at fixed Xe current density for two irradiation temperatures are shown in Fig. 1. The ratio of

[a] Permanent address: Shanghai Institute of Metallurgy, Academy of Sciences of China, Shanghai, China.

 0021-8979/86/093077-04$02.40 © 1986 American Institute of Physics

Downloaded 22 Dec 2005 to 131.215.225.9. Redistribution subject to AIP license or copyright, see http://jap.aip.org/jap/copyright.jsp

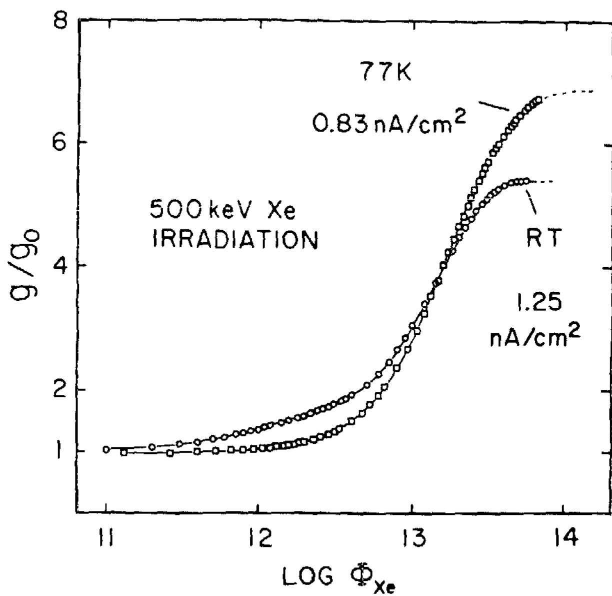

FIG. 1. Change in relative $CrSi_2$ film conductance $g(\phi)/g_0$ vs fluence ϕ, measured *in situ*, for 500-keV Xe irradiation at RT and 77 K.

conductance after fluence ϕ to initial conductance $g(\phi)/g_0$ is plotted semilogarithmically versus fluence ϕ for 500-keV Xe irradiations. The behavior is similar for other energies and ions. No significant substrate dependence was observed (correcting for background substrate conduction in $CrSi_2$ films grown on the $p<111>$ Si substrates).

The Hall effect measurements do not reveal a substantial change in the magnitude of the Hall mobility for Xe fluences below 10^{14} cm^{-2}, although there is an apparent conversion to predominantly n-type conductivity at fluences exceeding 10^{12}–10^{13} cm^{-2}.

It was observed in *in situ* experiments that at room temperature, though not at 77 K, the film conductiviy decreases by 1–5% over a 20–60 s period after suspending irradiation. The temperature coefficient of resistivity is positive in this temperature range and cannot explain this change. Additionally, the magnitude and time scale are not consistent with thermal decay. Some self-annealing apparently occurs at room temperature.

IV. DISCUSSION

Our observations suggest that the enhancement of $CrSi_2$ conductivity results primarily from an increase in free-carrier concentration. We speculate that these carriers, possibly electrons, arise from completely ionized defects produced by the irradiation. The high mobility we observe (~ 10 cm^2/V s) relative to $\mu_n = 0.15$ cm^2/V s for electrons[4] suggests conduction via an impurity band. Figure 2 shows the variation in film resistivity with temperature before and after the LNT irradiation. The cooling curve is consistent with previous reports.[5] Carrier freeze-out is not an interference in this experiment.

The curves of g/g_0 vs ϕ exhibit a simple structure at high fluences ($>10^{13}$ cm^{-2}), indicating that a first- or possibly second-order process may be responsible for saturation.[8] This suggests plotting $d(g/g_0)/d\phi$, which was calculated using three-point Lagrangian interpolation, versus g/g_0, as

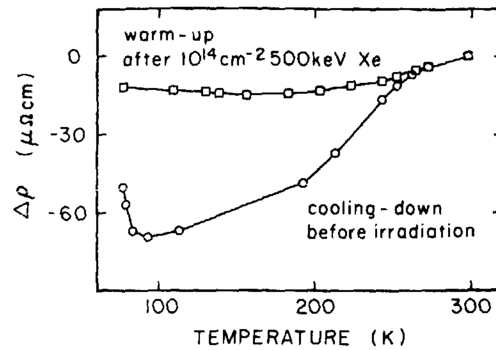

FIG. 2. Graph of resistivity change *relative to RT value* vs temperature for $CrSi_2$ film before and after irradiation at 77 K with 10^{14} cm^{-2}, 500-keV Xe.

shown in Fig. 3 for samples implanted with 500 keV Xe at room temperature, 77 K, and with 150-keV Ar. The results for all *in situ* room-temperature implantations display similar behavior. All of the curves have a similar shape for $g/g_0 > \sim 2$, independent of temperature. One mechanism probably dominates this regime. Considering the behavior for $g/g_0 < \sim 2$, there appears to be an additional process present during RT irradiation which is suppressed at 77 K. It is evident from Fig. 3 that there is a nearly linear relationship

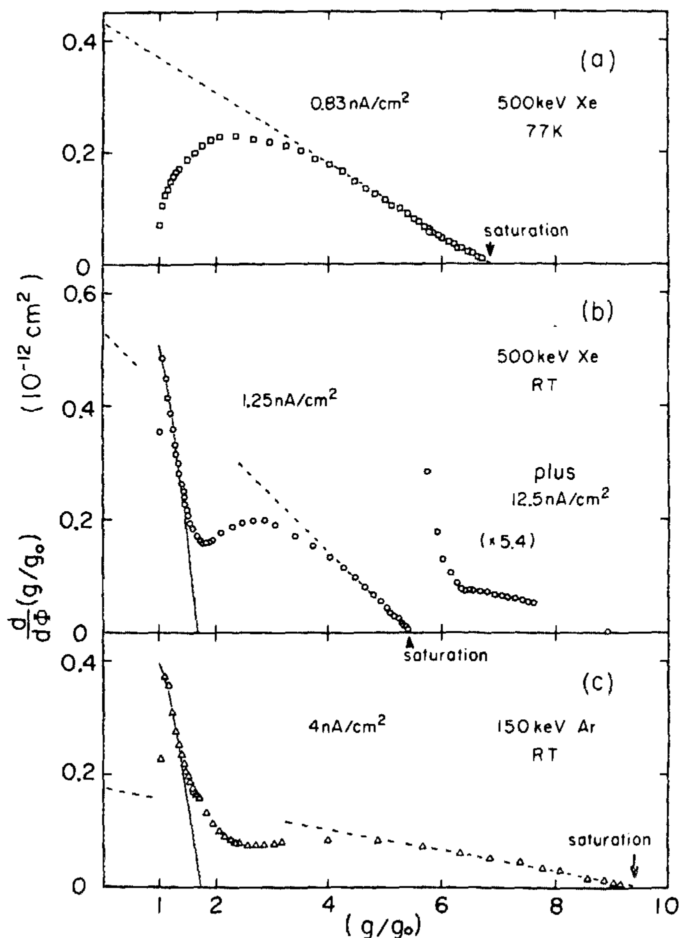

FIG. 3. Graph of $d(g/g_0)/d\phi$ vs (g/g_0) for 500-keV Xe irradiation at 77 K, RT and for 150-keV Ar at room temperature: (a), (b), and (c) respectively. In (b), the Xe current density was increased to 12.5 nA/cm^2 after saturation had occurred at 1.25 nA/cm^2 for a dose of $\sim 10^{15}$ Xe cm^{-2}.

Downloaded 22 Dec 2005 to 131.215.225.9. Redistribution subject to AIP license or copyright, see http://jap.aip.org/jap/copyright.jsp

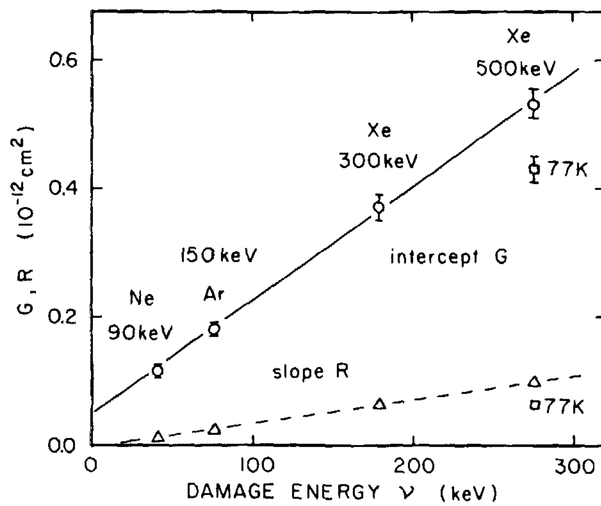

FIG. 4. Graph of intercept G and slope R vs damage energy ν for various ion-energy combinations studied.

between $d(g/g_0)/d\phi$ and (g/g_0) as they approach zero and saturation, respectively:

$$\frac{d}{d\phi}\left(\frac{g}{g_0}\right) = G - R\left(\frac{g}{g_0}\right). \tag{1}$$

In Fig. 4 we plot the values of G and R derived from this asymptotic dependence (dashed lines in Fig. 3) versus the deposited damage energy ν for the various ion-energy combinations studied.[7] The predominately linear dependence suggests that G corresponds to the generation of defects by the incident ion's nuclear energy loss, while existing defects recombine via radiation-enhanced diffusion.[9,10] The typical influence of dose rate on damage in $CrSi_2$ is demonstrated in Fig. 3(b). Further increases in g/g_0 were produced after saturation was reached ($\phi \simeq 10^{15}$ cm^{-2}) at a Xe current density of 1.25 nA/cm^2 by raising the current to 12.5 nA/cm^2. This effect requires further systematic investigation.

Simple models of overlapping coverage[10,11] are not adequate to describe the saturation at high fluences. However, they may be pertinent to the room- temperature behavior in Figs. 3(b) and 3(c) for $g/g_0 < 2$. If an incident ion produces an initial change in conductivity which is large compared to that produced by subsequent overlapping cascades, then $d(g/g_0)/d\phi$ would decrease substantially when $a\phi \gg 1$, where (a) is the effective area of the initially modified region. The solid lines in Figs. 3(b) and 3(c) correspond to such a model, assuming that subsequent impacts produce no additional change (see Appendix). By fitting these lines to the data, we deduce effective areas of $(8.7)^2$, $(10)^2$ nm^2 for 150-keV Ar, 500-keV Xe irradiation, respectively. The areas corresponding to transverse damage straggling $\pi \langle y^2 \rangle_D$ are $(33)^2$, $(44)^2$ nm^2, respectively, using Winterbon's calculations.[7] Recent studies of ion irradiation damage in tungsten using field ion microscopy[12] show that the average radius of the damaged region is $\sim 0.25 \langle y^2 \rangle_D^{1/2}$. These results show that our estimates of (a) are quite reasonable. The fact that the initial transient vanishes at 77 K indicates that the initial process occuring at RT involves defect diffusion and/or complex formation. The defects may not be sufficiently mobile at 77 K to produce this effect. This reduced mobility of defects may also account for the reduced values of G and R at 77 K in Fig. 4. The slight initial reduction in conductivity for fluences below 10^{11} cm^{-2} is accordant with this model of localized damage, since a reduction in carrier (hole) mobility due to scattering from these dispersed regions may dominate at very low fluences.

The 77 K result shown in Fig. 3(a) suggests that an electrically active compound defect is responsible for the increase in film conductivity. A significant feature is that $d(g/g_0)/d\phi$ initially starts near zero and increases very rapidly with respect to (g/g_0). This indicates that other electrically inactive defects are formed first and subsequently lead to formation of the active defect. The behavior at 77 K can be explained formally by the following model. We assume that the formation of the active defect A is limited by the formation of a simple inactive precursor defect I. All other intermediaries are assumed to be steady state, and competing reactions are neglected. The model can be described by the coupled reactions

$$0 \underset{(k_2)}{\overset{(k_1)}{\rightleftharpoons}} \{?\} + I, \tag{2a}$$

$$I + \{?'\} \underset{(k_4)}{\overset{(k_3)}{\rightleftharpoons}} A, \tag{2b}$$

where $\{?\}$ and $\{?'\}$ refer to unspecified defects. In this case quasi-first- order chemical kinetics apply, and the corresponding concentrations C_a (ϕ), C_i (ϕ) follow[13]:

$$\frac{d}{d\phi}C_i = k_1 - k_2 C_i - \frac{d}{d\phi}C_a, \tag{3}$$

$$\frac{d}{d\phi}C_a = k_3 C_i - k_4 C_a, \tag{4}$$

where the empirical rate constants k_1, k_2, k_3, k_4 depend on ion flux $d\phi/dt$, deposited energy ν, steady-state densities of other defects, etc. $g - g_0$ is assumed proportional to C_a; $(g/g_0) - 1 = \beta C_a$. The solution of Eqs. (3) and (4) for $C_i(0) = C_a(0) = 0$ gives

$$C_a(\phi) = \frac{(k_1 k_3)}{pq}\left(1 - \frac{pe^{-q\phi} - qe^{-p\phi}}{p - q}\right), \tag{5}$$

where

$$p,q = \frac{k_2 + k_3 + k_4}{2} \pm \left[\left(\frac{k_2 + k_3 + k_4}{2}\right)^2 - k_2 k_4\right]^{1/2}.$$

There are three relevant empirical parameters; $(\beta k_1 k_3)$, p, and q. We assume $p \neq q$. The asymptotic behavior for this model is

$$\frac{d}{d\phi}C_a \sim \left(\frac{k_1 k_3}{p}\right) - qC_a, \quad \text{as } \phi \to \infty, \tag{6a}$$

and as $\phi \to 0$;

$$\frac{d}{d\phi}C_a \sim (2k_1 k_3 C_a)^{1/2}\left[1 - \left(\frac{p+q}{3}\right)\left(\frac{2C_a}{k_1 k_3}\right)\right]^{1/2}, \tag{6b}$$

which is clearly the desired behavior. Figure 5 shows the result of fitting this simple model (solid line: $\beta k_1 k_3 = 9.01 \times 10^{-26}$ cm^4, $q = 0.064 \times 10^{-12}$ cm^2, $p = 0.24 \times 10^{-12}$ cm^2) to the results of Fig. 3(a). The agreement is excellent, although only suggestive. Variations of this model may also fit equally as well. A physical model requires knowledge of $CrSi_2$ defect chemistry which is lacking at

Downloaded 22 Dec 2005 to 131.215.225.9. Redistribution subject to AIP license or copyright, see http://jap.aip.org/jap/copyright.jsp

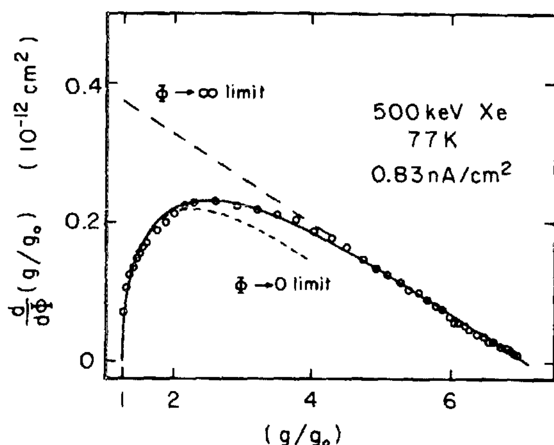

FIG. 5. Result of fitting simple coupled reaction model Eq. 5, (solid line) to 77 K Xe irradiation data (open circles) from Fig. 2(a). Asymptotic behavior is shown by dashed lines [from Eqs. 6(a), 6(b)].

present. It is likely that k_1 follows a Kinchen–Pease dependence (e.g., nearly linear in damage energy ν).[14] General statements about the other rate constants are not so obvious.

V. CONCLUSIONS

Our preliminary investigations have revealed a substantial amount of structure in the fluence dependence of inert ion implantation on $CrSi_2$ conductivity. Several processes seen in other systems have been tentatively identified. Electrical measurements provide a good qualitative characterization, but are relatively nonspecific and nonunique in their interpretation. Structural analysis from TEM, etc., is essential. The defect chemistry of $CrSi_2$ needs to be considered. The thermal annealing behavior of implanted $CrSi_2$ may offer some insight. Further investigation of irradiation damage in $CrSi_2$ at very low fluences ($\sim 10^{10}\ \mathrm{cm}^{-2}$) shows promise in elucidating the damage process, especially with light ions (e.g., Ne). $CrSi_2$ may be a good material to use in the study of dose rate effects.

ACKNOWLEDGMENTS

We thank A. Ghaffari for assistance with the evaporations and A. Collinwood for manuscript preparation. We acknowledge the partial financial support by the Office of Naval Research under Contract no. N00014-84-K-0275 (D. Polk). T. Banwell thanks IBM for a fellowship during this work.

APPENDIX

The effective conductivity of a two-dimensional medium composed of a random arrangement of regions with conductivities σ_0 and $b\sigma_0$ with fractional coverage $1-p, p$, respectively can be approximated by[15]:

$$y^2 - y(2p-1)(b-1) - b = 0,$$

where $y = \sigma/\sigma_0$. In our problem $p = 1 - \exp(-a\phi)$ is the fraction of area involved in at lease one cascade and possessing conductivity $b\sigma_0$. Differentiating and rearranging gives

$$\frac{d}{d\phi} y = a(b-y)\left(\frac{y^2+y}{y^2+b}\right).$$

The values of b used in Figs. 3(b) and 3(c) were determined by trial and error, with $b = 1.67$ and 1.71, respectively, producing reasonable agreement with the experiment.

[1] J. C. Hensel, R. T. Tung, J. M. Poate, and F. C. Unterwald, Nucl. Instrum. Methods (in press).
[2] C. A. Hewett, I. Suni, S. S. Lau, L. S. Hung, and D. M. Scott, in *Ion Implantation and Ion Beam Processing of Materials*, Vol. 27, edited by G. K. Hubler, O. W. Holland, C. R. Clayton, and C. W. White (North-Holland, New York, 1984), p. 145.
[3] U. Shreter and J. Nuchols (unpublished).
[4] M-A. Nicolet and S. S. Lau, in *VLSI Electronics: Microstructure Science*, Vol. 6, edited by N. Einspruch and G. Larrabee (Academic, New York, 1983), p. 391.
[5] F. Nava, T. Tien, and K. N. Tu, J. Appl. Phys. **57**, 2018 (1985).
[6] L. J. Van der Pauw, Phillips, Res. Rep. **13**, 1 (1958).
[7] K. B. Winterbon, *Ion Implantation Range and Energy Deposition Distributions* (IFI Plenum, New York, 1975).
[8] R. C. Birtcher, R. S. Averback, and T. H. Blewitt, J. Nucl. Mater. **75**, 167 (1978).
[9] G. J. Dienes and A. C. Damask, J. Appl. Phys. **29**, 1713 (1958).
[10] R. Webb and G. Carter, Radiat. Effects **42**, 159 (1979).
[11] R. P. Webb and G. Carter, Radiat. Effects **59**, 69 (1981).
[12] C-Y. Wei, M. I. Current, and D. N. Seidman, Philos. Mag. A **44**, 459 (1981).
[13] R. Sizmann, J. Nucl. Mater. **67–70**, 386 (1980).
[14] B. M. Paine and B. X. Liu, in *Materials Surfaces, Part A: Modification*, edited by C. R. Clayton and J. B. Lumsden (Academic, New York), (in press).
[15] S. Kirkpatrick, Phys. Rev. Lett. **27**, 1722 (1971).

Downloaded 22 Dec 2005 to 131.215.225.9. Redistribution subject to AIP license or copyright, see http://jap.aip.org/jap/copyright.jsp